Aerosol characteristics observed in southeast Queensland and implications for cloud microphysics

Sarah A. Tessendorf,[1] Courtney E. Weeks,[1] Duncan Axisa,[1] and Roelof T. Bruintjes[1]

Received 20 August 2012; revised 13 February 2013; accepted 14 February 2013; published 4 April 2013.

[1] Regular cloud base aerosol measurements were collected by a research aircraft over a 4 month period during the wet season in southeast Queensland, near Brisbane, Australia. In situ cloud microphysical measurements were also collected in many of these clouds. Brisbane is situated on the east coast of Australia and, depending on the synoptic weather conditions, can experience influences from inland or from the adjacent ocean. In situ aerosol measurements were used to compile a climatology of the aerosol conditions in the region and a back trajectory model was run for 120 h from each measurement to determine the possible air mass influences on each measurement. The most influential factor on the measured aerosol concentrations was the time the trajectory spent over land beneath 2 km (a proxy for the boundary layer). Using this criterion, the measurements were divided into two regimes: maritime for those with minimal time histories over land and continental for the remainder. Other influential factors on the aerosol concentration were also diagnosed and quantified with a regression model, including the proximity of the trajectory to the city of Brisbane and the number of fires along the trajectory. Thermodynamic, aerosol, and cloud microphysical characteristics are presented for each regime. The maritime regime tended to have more coarse mode (larger) aerosol particles and a tail of larger drops in the cloud base droplet spectra, which could be due to nucleation on the larger aerosol particles. The city influence on maritime regime trajectories yielded enhanced nucleation (fine) particle concentrations.

Citation: Tessendorf, S. A., C. E. Weeks, D. Axisa, and R. T. Bruintjes (2013), Aerosol characteristics observed in southeast Queensland and implications for cloud microphysics, *J. Geophys. Res. Atmos.*, *118*, 2858–2871, doi:10.1002/jgrd.50274.

1. Introduction

[2] Understanding the influence of aerosol on cloud microphysics and precipitation formation is of great importance, especially since such effects are potentially large yet not well understood [*IPCC*, 2007]. While it is well established that aerosols are necessary for cloud droplet nucleation and that as such aerosols could affect precipitation formation [*Feingold et al*., 1999; *Freud et al*., 2008; *Hudson et al*., 2009, 2011], it is still not well understood to what extent subsequent precipitation growth is affected by aerosol-influenced droplet spectra, especially in deep convection [*Squires*, 1958; *Rosenfeld*, 1999, 2000; *Khain et al*., 2005; *Tao et al*., 2007; *Rosenfeld et al*., 2008]. For example, in clean environments with low concentrations of cloud condensation nuclei (CCN), initial droplet spectra are often broader than in more polluted environments. A broader droplet spectra should, in theory, lead to more efficient collision and coalescence processes, whereas a narrow spectra could reduce that efficiency. Nonetheless, there are many other factors that can influence precipitation processes, including thermodynamic and dynamic variables.

[3] A recent study by *Bigg* [2008] concentrated on this issue for the region of southeast Queensland, Australia, by speculating that urban pollution could be related to the decrease in rainfall that this region had faced in the prior 35 years. *Bigg* [2008] stated, however, that "the present concentrations of potentially precipitation-influencing particles is not known at any site or for any season [in Australia]." As such, physical relationships between precipitation-influencing aerosol and rainfall in the region cannot be established. This paper presents such in situ aerosol measurements, for the southeast Queensland region, that were collected during the Queensland Cloud Seeding Research Program (QCSRP) [*Tessendorf et al*., 2010, 2012].

[4] A good understanding of the natural aerosol present in the atmosphere and its effect on cloud droplet formation is paramount toward understanding implications on precipitation formation in a given region. The goal of this study is to define the typical aerosol regimes observed in southeast Queensland and present representative characteristics of each regime. Such representations can be used for further detailed study of the precipitation processes in the region, including initializations for cloud resolving microphysical models.

[1]National Center for Atmospheric Research, Boulder, Colorado, USA.

Corresponding author: S. A. Tessendorf, National Center for Atmospheric Research/Research Applications Laboratory, P.O. Box 3000, Boulder, CO 80307, USA. (saraht@ucar.edu)

2169-897X/13/10.1002/jgrd.50274

2. Data Set and Methods

[5] The measurements discussed herein were collected during the QCSRP between November 2008 and February 2009 in southeast Queensland, Australia. All measurements were collected over land, surrounding the Brisbane metropolitan area (see Figures 1 and 3 in *Tessendorf et al.* [2012] for a map of the region and the flight tracks). The South African Weather Service Aerocommander was flown into and around clouds in the region equipped with a suite of microphysical instruments to obtain measurements of aerosol and droplet size spectra (see Table 1). Fine mode aerosol measurements were made with an aircraft-based high flow rate automated differential mobility analyzer (DMA) system [*Collins et al.*, 2000]. The scanning DMA data were processed using a fixed voltage transfer function [*Collins et al.*, 2004]. Accumulation mode aerosol were measured by a Passive Cavity Aerosol Spectrometer Probe (PCASP) and when out of cloud a Forward Scattering Spectrometer Probe (FSSP) [*Dye and Baumgardner*, 1984] was used to measure coarse mode (>3 μm) particles (Table 1). However, it should be noted that the FSSP has sampling limitations in measuring coarse particles that are often present in very low concentrations and the FSSP was always run in cloud droplet size range mode (see Table 1) since it was primarily used to measure cloud droplet spectra. FSSP instruments measure particles at ambient relative humidity and, depending upon the fraction of hygroscopic particles, may measure a mixture of wet and dry particles. The combination of low sampling statistics in the FSSP and complex refractive index due to a mixture of wet and dry particles introduces uncertainty in the size assignment by the FSSP. On the other hand, the sampling process of the PCASP and DMA instruments measure particles after most of the water has dried. The PCASP and FSSP were calibrated using latex spheres and glass beads, respectively, of known size and refractive index, and each was operated with 30 separate size bins using the Signal Processing Package (SPP) electronics (SPP-100 for the FSSP and SPP-200 for the PCASP) from Droplet Measurement Technologies (DMT).

[6] A DMT single column Cloud Condensation Nuclei (CCN-100) counter [*Roberts and Nenes*, 2005] was used with a constant pressure controller unit to keep the CCN sample at a constant pressure of approximately 600 hPa. Measured CCN concentrations were then corrected to ambient pressure [*Roberts and Nenes*, 2005]. A Cloud Imaging Probe (CIP; on a CAPS instrument, see *Baumgardner et al.* [2001]) and a Precipitation Imaging Probe (PIP) were used to measure the size, shape, and concentrations of cloud and precipitation particles. The CIP and PIP were calibrated using their respective spinning disk calibration tools.

[7] To sample subcloud aerosol near cloud base (hereafter, "cloud base aerosol"), the aircraft orbited below solid cloud bases that were at least 2 km in diameter with a 2 m s^{-1} or greater updraft as detected by the pilots, maintaining a

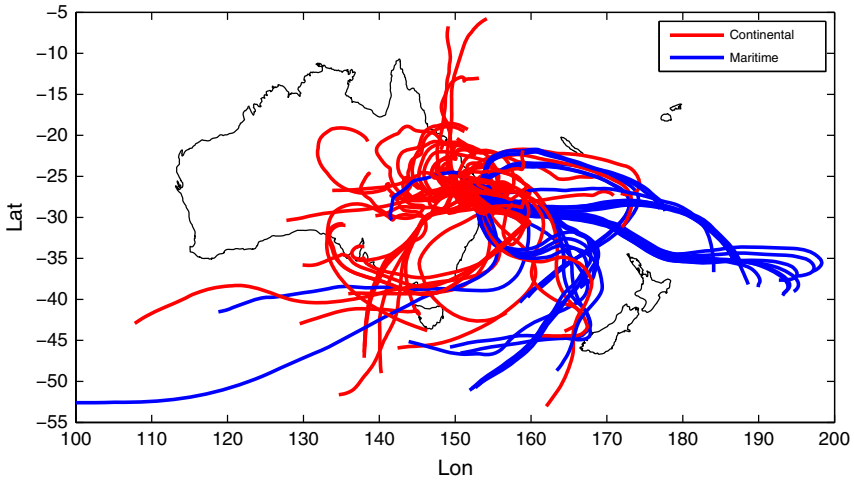

Figure 1. 120 h HYSPLIT back trajectories for each cloud base aerosol measurement color-coded into two regimes based on how much time each trajectory spent over land below 2 km: (blue) maritime regime ≤ 12 h and (red) continental regime > 12 h.

Table 1. List of Instrumentation Used to Take Measurements Discussed Herein. [a]All of the instruments except the DMA were models from Droplet Measurement Technologies (DMT)

Instrument	Purpose	Range
CCN Counter	Cloud condensation nuclei concentration and spectra	Depends on supersaturation
DMA	Fine mode aerosol spectra and concentration	0.01–0.38 μm
SPP-200 PCASP	Aerosol concentration and spectra	0.1–3 μm
SPP-100 FSSP	Coarse mode aerosol spectra	3–47 μm
CIP	Cloud particle size, shape, concentration	25–1500 μm
PIP	Precipitation particle size, shape, concentration	100–6200 μm

constant altitude and remaining in the updraft as much of the time as possible. In order to remain below the cloud, the aircraft orbits drifted with the cloud. Cloud base aerosol sampling orbits typically were on the order of 5 min, except when CCN supersaturation (SS) cycles were being run, in which case the aircraft maintained the cloud base orbit for 10 min to allow for the CCN counter to sample at three supersaturations (0.3%, 0.5%, and 0.8%). The CCN counter was set to sample at 0.3% supersaturation at all other times. Statistics on cloud base aerosol measurements used in this analysis (median PCASP concentrations, median 0.3% SS CCN concentrations, and mean aerosol size spectra) were then calculated for a 3 min segment with relatively constant PCASP concentrations during each cloud base orbit. This allowed for a full up and down sizing cycle by the DMA to be represented in each measurement.

[8] After obtaining a cloud base aerosol sample, the aircraft typically ascended to collect measurements of the initial cloud droplet spectra at roughly 300 m above cloud base. Terrain occasionally impacted the aircraft's ability to fly in cloud at this altitude, and thus, the aircraft would ascend to its minimum safe altitude to conduct these "cloud base" passes. For the analysis presented herein, we only considered passes within 300–600 m of cloud base as "cloud base" passes and only for untreated clouds. Since this research was conducted as part of a cloud seeding research project, roughly half of the sampled clouds were treated with hygroscopic particles in a randomized cloud seeding experiment, thereby reducing the number of in-cloud measurements available for this analysis. Furthermore, we avoided data from portions of cloud passes through cloud edges or areas with precipitation by focusing on FSSP measurements with minimum concentrations of 20 cm^{-3} and excluded measurements with nonzero counts of particles larger than 100 μm as measured by the CIP and PIP.

2.1. Back Trajectory Modeling

[9] The Hybrid Single-Particle Lagrangian Integrated Trajectory (HYSPLIT) model [*Draxler and Rolph*, 2010] was used to calculate 120 h back trajectories in order to get an air mass history for each measurement. The model was run using the Global Data Assimilation System (GDAS) archived data, with a temporal resolution of 3 h and spatial resolution of 1° × 1° in latitude and longitude. The GDAS data set was the highest resolution set available for HYSPLIT that covered the project domain at the time of the measurements. Sensitivity tests of trajectories calculated using GDAS and other data sets [i.e., National Centers for Environmental Prediction (NCEP)/National Center for Atmospheric Research (NCAR) Reanalysis and Final Analyses (FNL)] for the same region in past years when those other data sets were available yielded highly similar results. The starting latitude, longitude, and altitude for each trajectory were based on the actual location of the aircraft while taking measurements. The back trajectories, shown in Figure 1, illustrate the wide variety of source regions.

[10] Since the aerosol characterization herein relies on the results of the HYSPLIT model run with GDAS data, a sensitivity study was performed to test the influence of the model data resolution and vertical motion calculation on the results. We recreated the results using the NCEP/NCAR Global Reanalysis Data (spatial resolution of 2.5° × 2.5° and 6 h output) with all other conditions held the same and again with the GDAS data, but computing vertical motion differently (isentropically rather than from modeled wind fields). Relationships of median PCASP concentration and hours over land, as calculated from these test runs, are shown in Figure 2, and will be discussed further in section 3.

3. Regime Classification

[11] Aerosol regimes were defined in this study using the modeled back trajectories for each of 69 cloud base aerosol measurements. Using the hours a trajectory spent over land within the boundary layer (2 km; hereafter, "hours over land") as a primary influential factor on the measured aerosol conditions, we determined that splitting the data set into two regimes produced significantly distinct aerosol regimes (in aerosol concentration, as well as aerosol size spectra): maritime, identified as ≤12 h over land below 2 km, and continental, with >12 h over land (see Figure 1). Using this classification, the broad range of PCASP concentrations

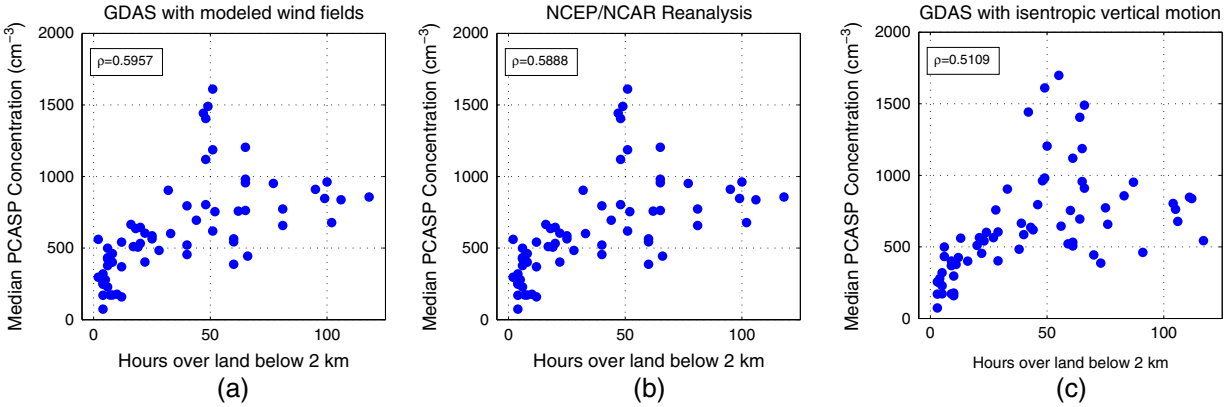

Figure 2. Sensitivity tests showing median PCASP concentration versus trajectory hours over land beneath 2 km as calculated using the (a) GDAS data set using modeled wind fields (as presented in rest of paper), (b) NCEP/NCAR Global Reanalysis Data using modeled wind fields, and (c) GDAS data using isentropically modeled vertical motion. The correlation coefficient (ρ) is noted for each panel.

measured in the season-wide data set can be partitioned into two distinct categories; however, there is still a fair amount of variability within each regime, especially the continental regime (Figure 3).

[12] The 12 h threshold determined by this analysis lies within the 95% confidence intervals for being the most significant regime threshold determined by the sensitivity tests with the reanalysis data and the isentropic vertical motion runs (see section 2.1). However, most notably from the lower resolution data run (Figure 2b), there are a few outlier points (low PCASP concentration, more time over land) that would be classified differently if NCEP/NCAR reanalysis were used to drive HYSPLIT instead of GDAS. Nonetheless, we feel that the results, in general, are robust and independent of the input data for HYSPLIT.

[13] These two regimes also exhibit distinctly different CCN concentrations, both at 0.3% supersaturation (Figure 3b) and for the other two supersaturations, on average, for those measurements with supersaturation cycles (Figure 4). Nonetheless, there is still considerable variability in the individual CCN SS cycle concentrations that will be explored in future analysis. However, those measurements with low (high) PCASP aerosol concentrations also tend to exhibit low (high) 0.3% SS CCN concentrations (Figure 5).

3.1. Other Influential Factors

[14] The variability in the measurements that still exists after classifying the regimes by the hours each trajectory spent over land can be explained by other influential factors, such as the number of fires along a trajectory, the proximity of the trajectory to the city of Brisbane (defined as the city center point at 27.5°S, 153.02°E), and the amount of rainfall in the 12 h period prior to the measurements. Fire locations and times were determined by the MODIS Fire and Thermal Anomalies Product [*Giglio et al*., 2003] and processed as in *Wiedinmyer et al*. [2006]. The number of fires along a trajectory (hereafter, proximity fires) was the number of MODIS fire locations within a 200 km radius of the trajectory at each hour along the 120 h back trajectory. This method may count the same fire multiple times, which implies that it had more time to influence the air mass. Rainfall was calculated from the GDAS model and accumulated along the last 12 h of the trajectory.

[15] For the maritime air masses, there was little relationship between aerosol concentrations and hours over land (Figure 6a); however, the maritime aerosol concentrations exhibited a considerable increase as the trajectories got

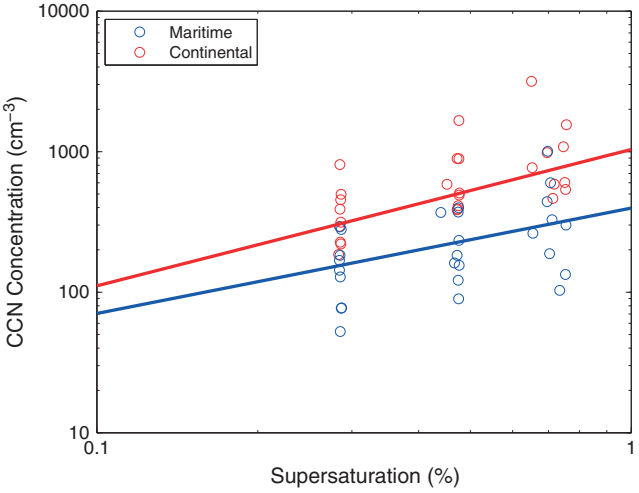

Figure 4. CCN concentrations at varying supersaturations measured during cloud base supersaturation cycles, colored by maritime (blue) and continental (red) regimes. The solid line represents the power law fit (based on equation (4)) for each regime. There is some scatter about the set supersaturation values, most notably around 0.8%, because temperatures did not actually stabilize in every cycle to achieve the specified supersaturation. Therefore, the temperature difference within the column was used to calculate the actual supersaturation for each measurement.

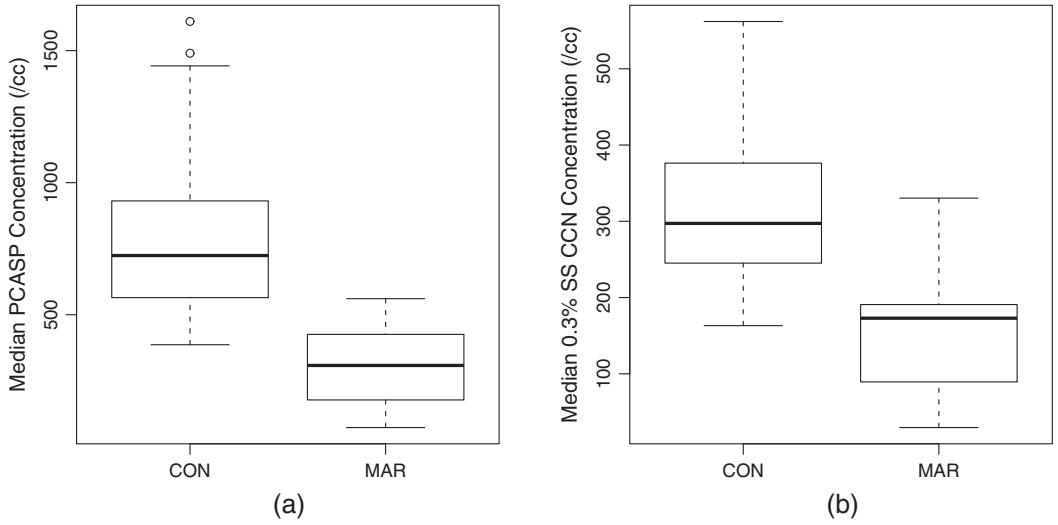

Figure 3. Box and whisker plots of (a) median PCASP aerosol concentration and (b) median 0.3% SS CCN concentration split by regime (MAR: ≤12 h over land below 2 km; CON: >12 h over land below 2 km).

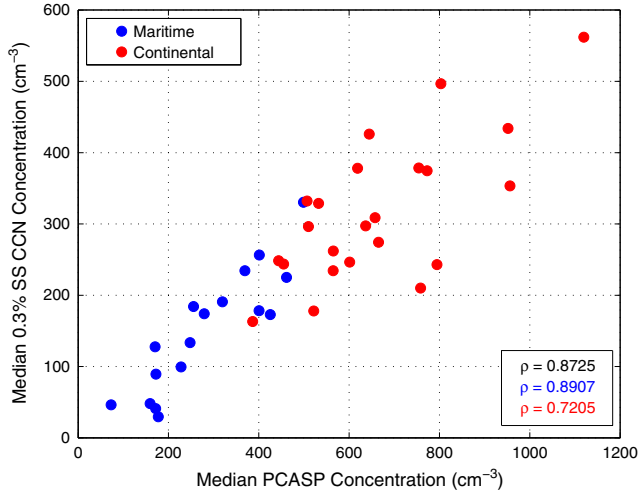

Figure 5. Scatter plot of the median PCASP concentration and 0.3% SS CCN concentration for each cloud base aerosol measurement, colored by (blue) maritime and (red) continental regimes. [Note that not all of the PCASP measurements used in the regime analysis had corresponding CCN measurements, given that the CCN instrument was not available on every flight. Thus, in this analysis with CCN measurements, the maritime (continental) regime had 21 (24) samples.] The correlation coefficient (ρ) is noted for each regime (color) and for all points combined (black).

closer to Brisbane (Figure 6b). Very few of the maritime cases were influenced by any fires; which is not surprising due to the relatively short time these trajectories spent over land (and therefore fewer opportunities to be near a fire) as well as because fires were more common in months when maritime flow trajectories were less common (Figure 7). November and December experienced far more fires, less rainfall along the trajectory prior to measurement, and generally more continental flow while the second half of the rainy season was more maritime in nature, with fewer fires and more rainfall along the trajectories. The fires in November and December were primarily from the sugar cane–harvesting season, the effects of which have been previously discussed in *Warner and Twomey* [1967] and *Warner* [1968].

[16] Conversely, the continental concentrations were highly dependent on the number of fires observed along the trajectory (Figure 6c), while showing some dependence on hours over land and no relationship with distance to Brisbane (Figures 6a and 6b). The lack of dependence on distance to Brisbane in the continental flow is unsurprising, given that the measurements collected in continental flow were inland from Brisbane and were more often made upwind of the city.

[17] Figure 6d illustrates how both regimes' aerosol concentrations were affected by recent rainfall. While noisy, the trend suggests that the concentrations will be lower with greater rainfall, as would be expected due to precipitation scavenging [e.g., *Kerker and Hampl*, 1974; *Barlow and Latham*, 1983].

[18] Trajectories and locations of fires throughout the 120 h duration of each trajectory are illustrated in Figure 8 for examples of two extreme aerosol concentration measurements. Figure 8a displays the highest PCASP concentration (1610 cm^{-3}) on 6 December 2008, while Figure 8b shows the cleanest case (PCASP concentration, 73 cm^{-3}) on 14 February 2009. The 6 December case spent 51 h over land, was in proximity to 2436 fires (this value does include multiple counts of the same fire) throughout its 120 h path, and had very little (1.2 mm) rainfall to scavenge aerosol prior to the measurement. The 14 February trajectory, on the other hand, spent only 4 h over land, did not come closer than 50 km from Brisbane, and had nearly 12 mm of rainfall in the previous 12 h before the measurement.

[19] Based on these additional influences on aerosol concentration, each regime was broken into two subregimes (Figure 9): a "city-influenced maritime" regime was defined for trajectories with ≤12 h over land below 2 km and at least one time step along the trajectory that was <50 km to Brisbane, while all the remaining maritime regime data points were classified in a "non-city-influenced maritime" regime, and a "fire-influenced continental" regime was defined for trajectories with >12 h over land below 2 km and >1000 proximity fires, while all the remaining continental regime data points were classified in a "non-fire-influenced continental" regime.

[20] The mean aerosol concentrations for the continental and maritime regimes, as well as their respective subregimes, are summarized in Table 2. A *t* test was performed to determine if the means in each regime and subregime were significantly different. The *t* test assumes a null hypothesis that two data sets are independent random samples from normal distributions with equal means and equal, but unknown, variances. The assumption of normality of PCASP concentrations within each regime was confirmed with the Lilliefors test [*Lilliefors*, 1967]. The *t* test between the overall maritime and continental regimes yielded a *p* value of 3.57×10^{-7}.

[21] Furthermore, splitting the PCASP data into the maritime and continental regimes reduced the overall variability in measured aerosol concentration (measured as a sum square deviation) by 58.5%. Splitting into subregimes reduced the variability in the maritime and continental regimes by another 39.8%.

3.2. Regression Model

[22] One goal of this characterization analysis is to be able to predict general aerosol concentrations, in the absence of in situ aerosol measurements, with a tool that is readily available (e.g., HYSPLIT is open source). Based on this analysis, various features related to the back trajectory for a given measurement could be used to predict the resulting aerosol concentration. Therefore, PCASP concentrations were regressed on the most relevant trajectory "predictor" variables (hours over land below 2 km, distance to Brisbane, number of fires, and prior 12 h accumulated rainfall). Two models were created and will be discussed below.

[23] As a first pass, we built a regression model that treated the data as if it were more homogeneous, even though we have seen that the maritime- and continental-influenced flows have different relationships to the predictor variables. Nonetheless, with this method, the following formula was produced to estimate the PCASP concentration:

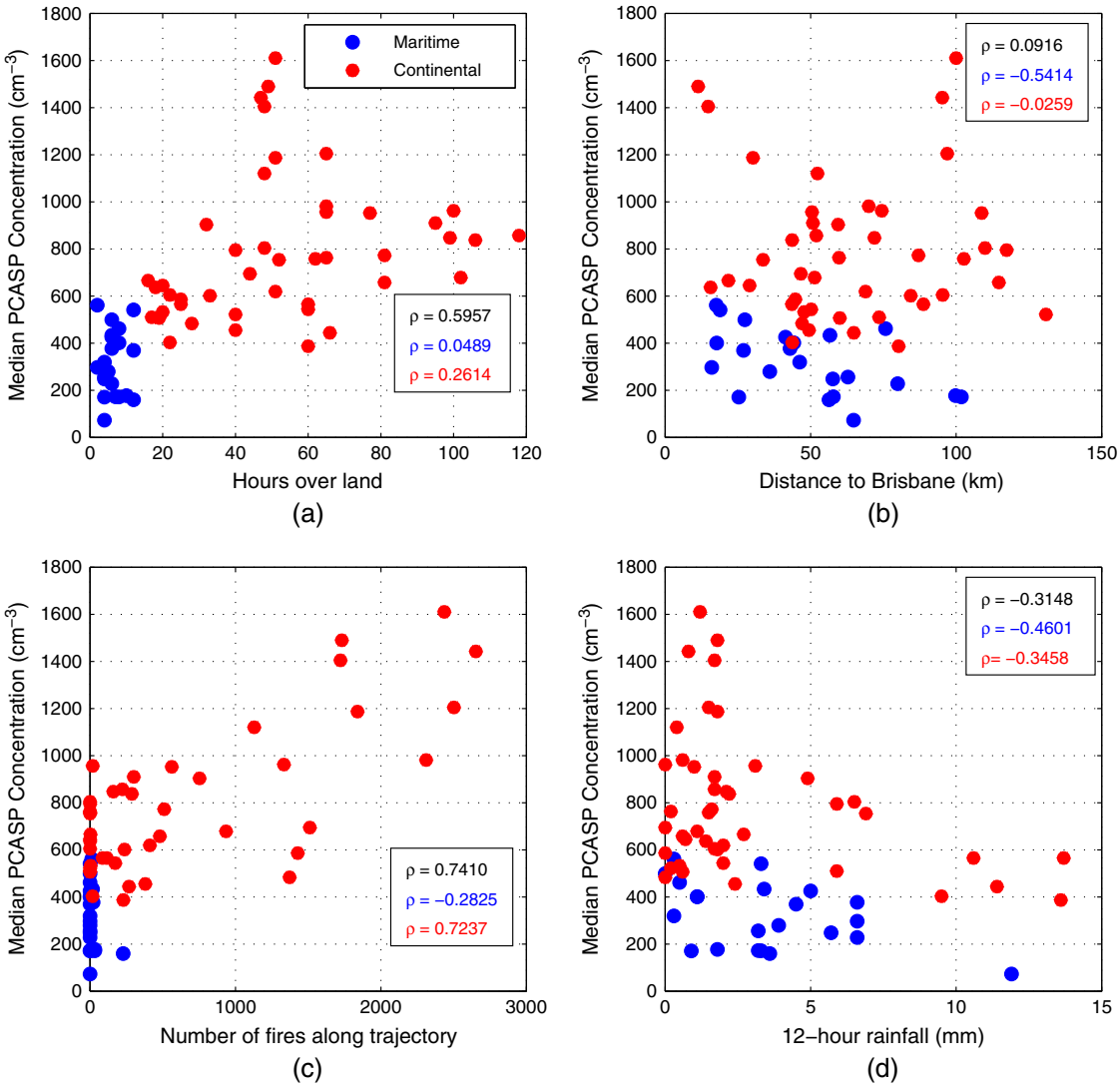

Figure 6. PCASP aerosol concentration variation based on the (a) hours over land below 2 km, (b) distance to Brisbane, (c) number of fires within 200 km of (and 12 h prior to) the trajectory, and (d) 12 h rainfall of each back trajectory colored by (blue) maritime and (red) continental regimes. The correlation coefficient (ρ) is noted (colored) for each regime and (black) for all points combined for each panel.

$$\text{PCASP\_est} = 361.10 + 4.01^{*}\text{HOLBL} + 0.28^{*}\text{Fires} \quad (1)$$

where "Fires" is the number of proximity fires and "HOLBL" is the hours the trajectory spent over land below 2 km. In this case, considering the whole data set as one population, neither distance to Brisbane nor recent rainfall was a significant predictor of the final aerosol concentration. The adjusted R^2 for this formula was 0.66.

[24] Based on the results of the aerosol characterization analysis, however, we do expect that the maritime and continental regimes may have different significant predictors. For example, the distance to Brisbane was more related to PCASP concentration for the maritime regime than it was for continental. Thus, we created a formula that takes the maritime versus continental regime classification into account. This formula produced the following relationship to estimate PCASP concentration:

$$\text{PCASP\_est} = 544.49 + C^{*}(0.24^{*}\text{Fires} + 2.41^{*}\text{HOLBL}) - M^{*}(3.02^{*}\text{DTB} - 22.60^{*}\text{Rain}) \quad (2)$$

where C = 1 (and $M = 0$) if HOLBL > 12 h (continental) and $M = 1$ (and $C = 0$) if HOLBL ≤ 12 h. In this relationship, "DTB" is the distance to Brisbane city center and "Rain" is the amount of modeled rainfall (mm) accumulated in the 12 h period prior to measurement time. The adjusted R^2 for this model was higher as we expected, at 0.71.

4. Regime Characteristics

4.1. Thermodynamic Environment

[25] In addition to differences in aerosol, there may be inherent environmental differences between these regimes that could affect cloud microphysics. Here we present a

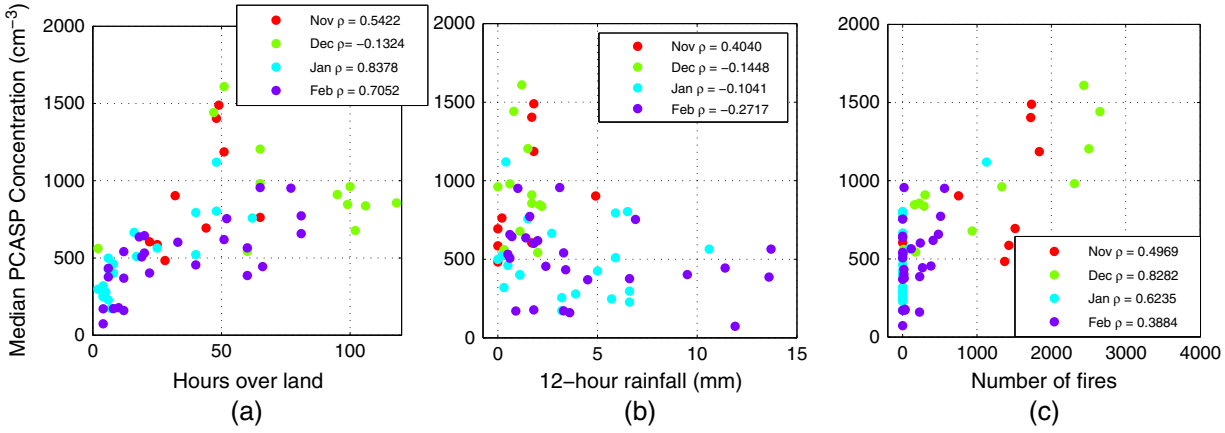

Figure 7. Monthly trends in concentration by hours over land below 2 km, rainfall, and number of fires (N = November, D = December, J = January, F = February). The correlation coefficient (ρ) is noted for each month (color) in each panel (note that ρ for all points combined is noted in Figures 6a–6c).

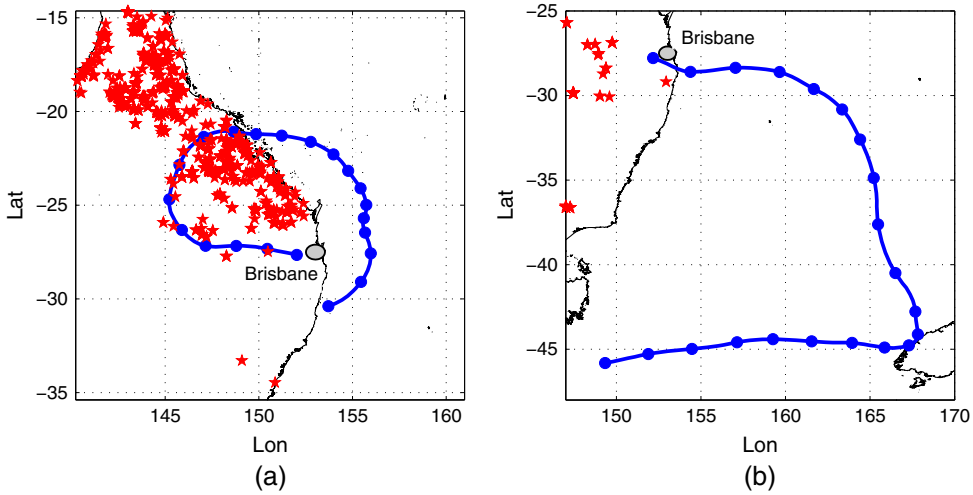

Figure 8. Trajectories corresponding to (a) the highest (6 December 2008) and (b) lowest (14 Febraury 2009) PCASP aerosol concentrations. Red asterisks represent the locations of fires within the 120 h trajectory period. The light gray-shaded region represents a 50 km radius around the Brisbane City center, for reference.

few factors, such as moisture and instability, to investigate this possibility (Figures 10–11). Cloud base heights were consistently lower in the maritime regime, suggesting more humid surface conditions, although average cloud base temperatures were quite similar between the two regimes. Average precipitable water was also fairly similar between the two regimes, although the continental regime exhibited variability that included colder cloud base temperatures and slightly higher precipitable water than the maritime regime.

[26] Instability is often measured by Convective Available Potential Energy (CAPE); however, CAPE is highly dependent on surface conditions that can temporally and spatially vary. Given that the 00Z soundings are taken at 10:00 A.M. local time, it was often the case that surface conditions measured by the sounding were not representative of the time of convection. Thus, here we present the Total Totals stability index [*Miller*, 1972] as well as CAPE values that were calculated using modified soundings to convective temperature. The Total Totals index is calculated as

$$\text{Total Totals} = t_{d850} + t_{850} - 2 \times t_{500} \quad (3)$$

where t_{d850} is the dew point at 850 hPa and t_{850} (t_{500}) is the temperature at 850 (500) hPa. Higher values indicate increased instability. Figure 10d indicates that both regimes have similar mean instability using this index. The continental regime, however, does exhibit a larger range of instability including slightly higher instability values. The modified CAPE values (Figure 11) continue to suggest that the continental regime often had higher *potential* instability than the maritime regime; however, we must note that convective temperatures were not always reached, especially for the continental regime, so these are just estimates of potential

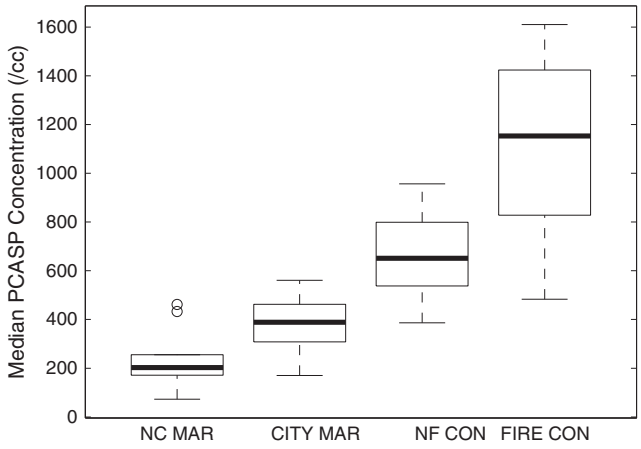

Figure 9. Box and whisker plots of median PCASP concentration for each of the subregimes: non-city-influenced maritime (NC MAR), city-influenced maritime (CITY MAR), non-fire-influenced continental (NF CON), and fire-influenced continental (FIRE CON). For sample sizes in each category, see Table 2.

Table 2. Regime and Subregime Mean Cloud Base PCASP Concentrations and Number of Measurements (N_obs) and the Number of Unique Days in Which the Measurements Were From (Days)

Regime	Subregime	Mean PCASP Concentration (cm^{-3})	N_obs	Days
Maritime	All	319	22	12
	Non-city-influenced	237.9	10	
	City-influenced	386.7	12	
Continental	All	786.6	47	17
	Non-fire-influenced	670.2	32	
	Fire-influenced	1097	15	

instability. Moreover, the vertical distribution of CAPE between the two regimes varied. For example, the total CAPE in the maritime regime was often limited by a trade wind subsidence inversion in the midlevels (see Figures 11c–11d). The CAPE values between 0 and 3 km were much more similar between the two regimes, although the maritime regime tended to have slightly more CAPE in this range (Figure 11b). The lower cloud base heights in the maritime regime may have contributed to this, allowing for more CAPE to occur below 3 km.

4.2. Aerosol Characteristics

[27] Aside from the significantly different PCASP (accumulation mode) aerosol concentrations discussed in section 3 that were used to help define the two regimes, the maritime and continental regimes also have unique features in the full aerosol size spectra created by combining measurements from the DMA, PCASP, and FSSP (Figure 12). Despite substantial variability in the measurements, the mean spectra highlight the tendency for the maritime regime to have a greater nucleation mode (<0.1 μm) of aerosol particles compared to the continental regime. Due to the extremely low concentrations of large particles measured by the FSSP, there is considerable noise in the coarse mode end of these spectra. Yet interestingly, the coarse modes (>3 μm) in both regimes are quite similar, although the maritime regime tends to have more coarse mode particles on average. Particle impactor samples indicated that most of the coarse mode particles analyzed, regardless of regime, were mineral dust [*Tessendorf et al*., 2012]. While this seems contrary to what one would expect for a maritime regime (in which sea salts often are more commonly attributed to the coarse mode), the fact that the maritime regime had lower cloud base heights could have allowed more of an influence from the land surface, even for the short duration that the trajectory spent over land prior to the measurement.

[28] When dividing into the four subregimes (Figure 13), some of the variability exhibited in Figure 12 is reduced. In particular, it is clear that the fire-influenced continental regime has a very weak coarse mode and an enhanced accumulation mode. Furthermore, the city-influenced maritime spectrum appears to be responsible for the enhanced nucleation mode particles observed in the maritime regime in Figure 12. In fact, the city-influenced maritime regime exhibits the highest nucleation mode concentrations of all four subregimes and also has enhanced accumulation particle concentrations compared to the non-city-influenced maritime regime (Figure 13). Particle impact samples analyzed on one such city-influenced maritime regime case (22 January 2009) indicated sulfur-bearing fine mode particles, similar to that measured in continental regime samples [*Tessendorf et al*., 2012].

4.3. Cloud Microphysics

[29] Initial ("cloud base") maximum droplet concentrations measured 300–600 m above cloud base should in theory be correlated with the aerosol that serve as CCN found at cloud base if they enter the cloud and become activated [*Hudson et al*., 2009, 2010]. However, taking in situ droplet measurements in cloud just above cloud base has several caveats, making it difficult to isolate the region of the cloud where you would expect the droplet measurements to be most related to the subcloud aerosol. Such issues are related to entrainment of cloud-free air, which dilutes the cloud water in the parcel below adiabatic conditions and typically affects cloud edges; drizzle and precipitation formation that may be falling from above, which may artificially broaden the drop spectra; and varying supersaturations in the cloud, in part due to varying updraft velocities, will also affect the number and sizes of particles that are activated. As described in section 2, we have done some processing of the data to omit measurements that may have been affected by precipitation (i.e., measurements having particles >100 μm on the CIP and PIP probes). Nonetheless, there are still several methods for characterizing the droplet concentrations in clouds, and each can yield different results [*Yum et al*., 1998; *Hudson and Yum*, 2001, 2002]. For example, one simple method is to calculate flight-averaged droplet concentrations, as has been done in some aerosol characterization studies; however, the cloud edge measurements will act to dilute the mean and would not provide the best measurements with which to compare the aerosol observations for individual clouds in the present study. Therefore, we aim to isolate measurements representative of the adiabatic core of the cloud. The maximum droplet

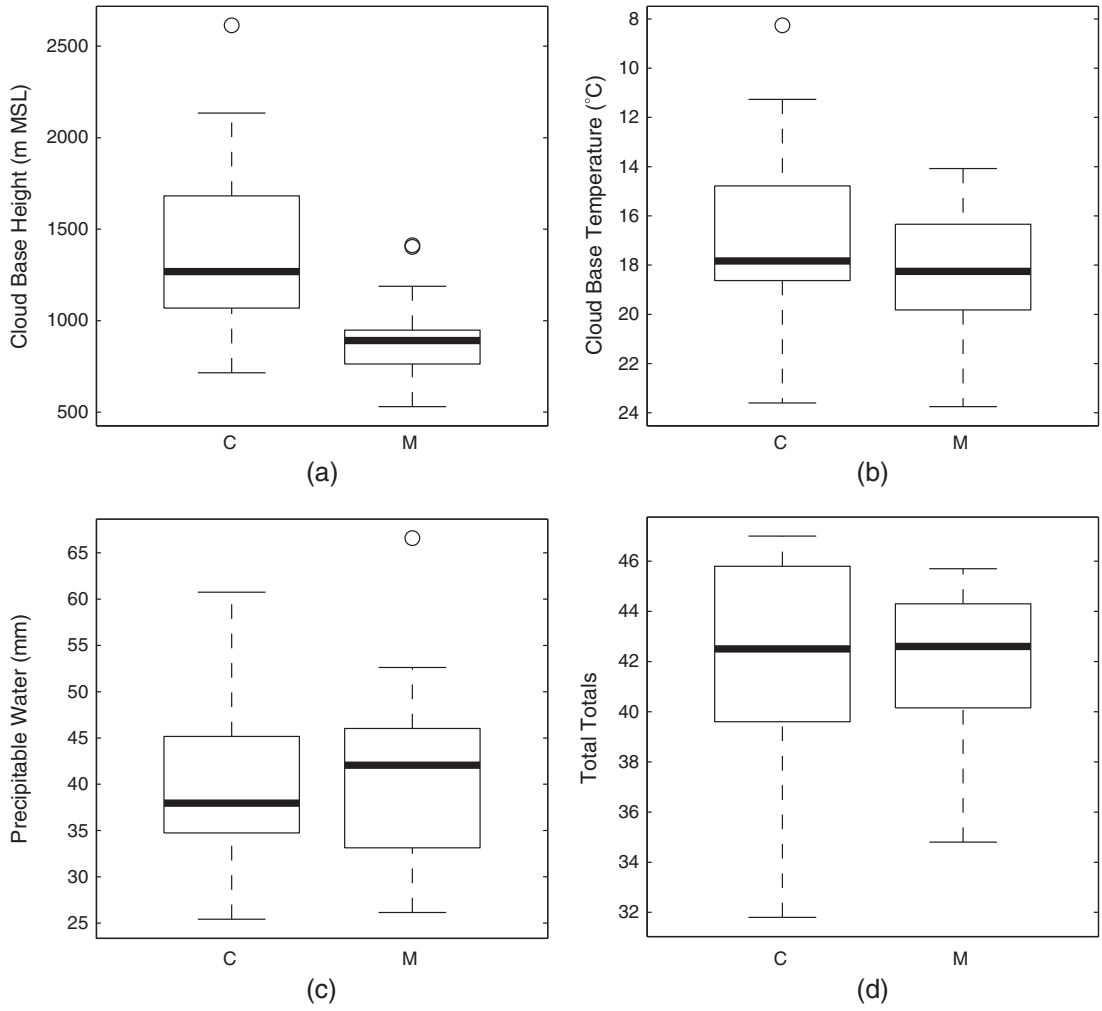

Figure 10. Box and whiskers plots of (a) cloud base height, (b) cloud base temperature, (c) precipitable water, and (d) the Total Totals stability index from 00Z Brisbane airport soundings on the day of each measurement.

concentration within a cloud pass should perform better for this purpose; however, absolute maximum measurements can be the result of artificial spikes in the data.

[30] Despite these challenges, we have attempted three different methodologies for calculating the typical droplet concentration, mean diameter, and size spectra just above cloud base that could result from nucleation on the aerosol particles that were measured below cloud base. Each method is described below, followed by a discussion of the results. As one may expect, each yielded different results, and we cannot speculate which is more correct, rather they are all possible scenarios that need to be considered.

4.3.1. Steady State Method

[31] This method is the most subjective of the three we utilized. Here we based the method on the principle that, when the aircraft is well inside the cloud and near the adiabatic core of the cloud, the liquid water content and drop concentrations should be fairly steady for a *minimum* of 3 s, which translates to roughly 250 m. Thus, these periods of level drop measurements were noted and means of the concentrations, mean diameter, and size spectra over the course of these steady periods were calculated for each cloud penetration.

4.3.2. Maximum Drop Concentration Method

[32] As stated earlier, in theory the maximum droplet concentration should be related to the subcloud aerosol. However, spikes that may occur in the 1-Hz data prevent this correlation from always being the case. Thus, we implemented an objective strategy that calculated the maximum droplet concentration in a given penetration and then took a mean of the concentration, mean diameter, and size spectra over the course of a 3 s period, plus or minus 1 s from the 1 Hz maximum measurement. This method ideally helped to smooth out spikes, but some of the 3 s averages may still have some influence from data spikes.

4.3.3. "Binmax" Method

[33] This method was presented in *Yum et al*. [1998] as an objective way to identify the near adiabatic droplet concentrations in cloud passes, while reducing the chances of contamination from spikes in the data. In their study, this method had high correlations of droplet and CCN concentrations; however, they included all cloud droplet measurements over a particular flight. In the present study, all 1 Hz droplet concentration measurements during passes through a particular cloud were binned into 10 cm^{-3} frequency

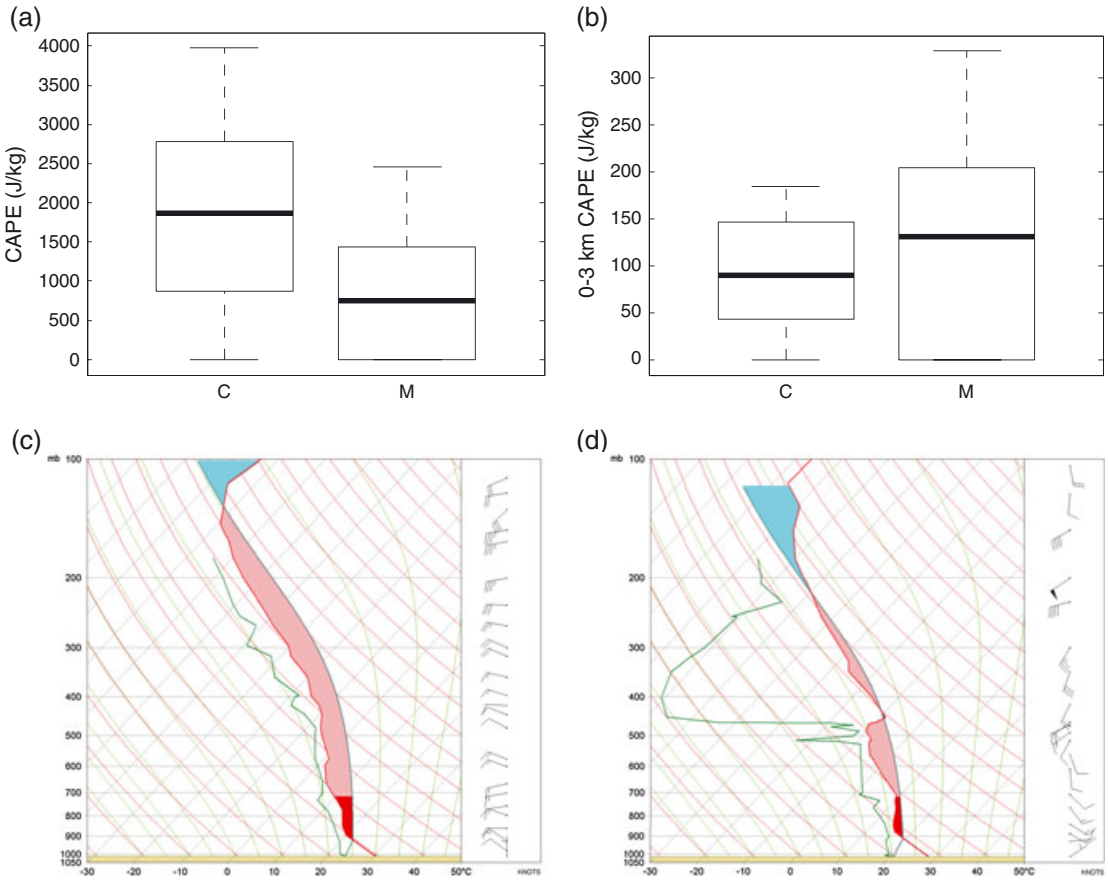

Figure 11. Comparison of Convective Available Potential Energy (CAPE) instability for the continental (C) and maritime (M) regimes and example sounding profiles from each regime. Box and whisker plots of (a) total CAPE, calculated at convective temperature, and (b) CAPE between 0 and 3 km, calculated at convective temperature. Sample soundings are from (c) 23 January 2009, a continental regime day, and (d) 26 January 2009, a maritime regime day.

distribution bins of droplet concentration. The data points in the bin with the highest concentration that also contained at least three 1-Hz data points were then used to calculate the droplet characteristics for that particular cloud. The droplet concentrations, mean diameters, and drop size spectra were then averaged from those data points in that maximum bin and used to represent the drop characteristics for the given cloud.

4.3.4. Cloud Base Droplet Characteristics

[34] Droplet concentration and mean diameter results using the steady state and maximum methods were very similar on average in both the maritime and continental regimes (Table 3), with the maximum method resulting in the highest drop concentration measurements, as may be expected. The similarities between the two regimes were peculiarly surprising given the marked differences in aerosol and CCN concentrations that had been observed. The "binmax" method yielded the most notable differences between the two regimes in a manner that would be expected given the lower (higher) aerosol concentrations and thus lower (higher) droplet concentrations in the maritime (continental) regime (Table 3). Mean droplet diameters were also larger in the maritime regime than the continental regime, which is also expected given the lower droplet concentrations and slightly broader aerosol size distributions in the maritime regime.

[35] Despite the similarities in droplet concentration between the regimes using the steady state and maximum methods, the cloud base droplet spectra did exhibit some slight differences in that, on average, the maritime spectra were generally broader due to a tail of larger droplets (Figure 14). This was also the case using the binmax method. This result was most notable in the steady state and binmax methods, in which the difference in the concentration of drops larger than 20 μm was statistically significant between the two regimes for both of these methods. The mean diameter was significantly different between the regimes (i.e., larger in the maritime regime) under the binmax method only. This tendency for a tail of larger drops in the maritime regime could be the result of droplet nucleation on larger aerosol particles (exhibited in the coarse mode of Figure 12).

[36] Comparing these results with cloud base droplet characteristics measured in extremely continental [*Fitzgerald and Spyers-Duran*, 1973; *Dye et al*., 1986] or truly maritime [*Hudson and Mishra*, 2007; *Hudson and Yum*, 2001, 2002] locations indicates that both regimes herein are really modified versions of what is traditionally "continental" or "maritime" (Figure 15). Recall that in this study all "maritime regime" measurements were indeed measured over land. However, these ranges of cloud base droplet measurements are fairly

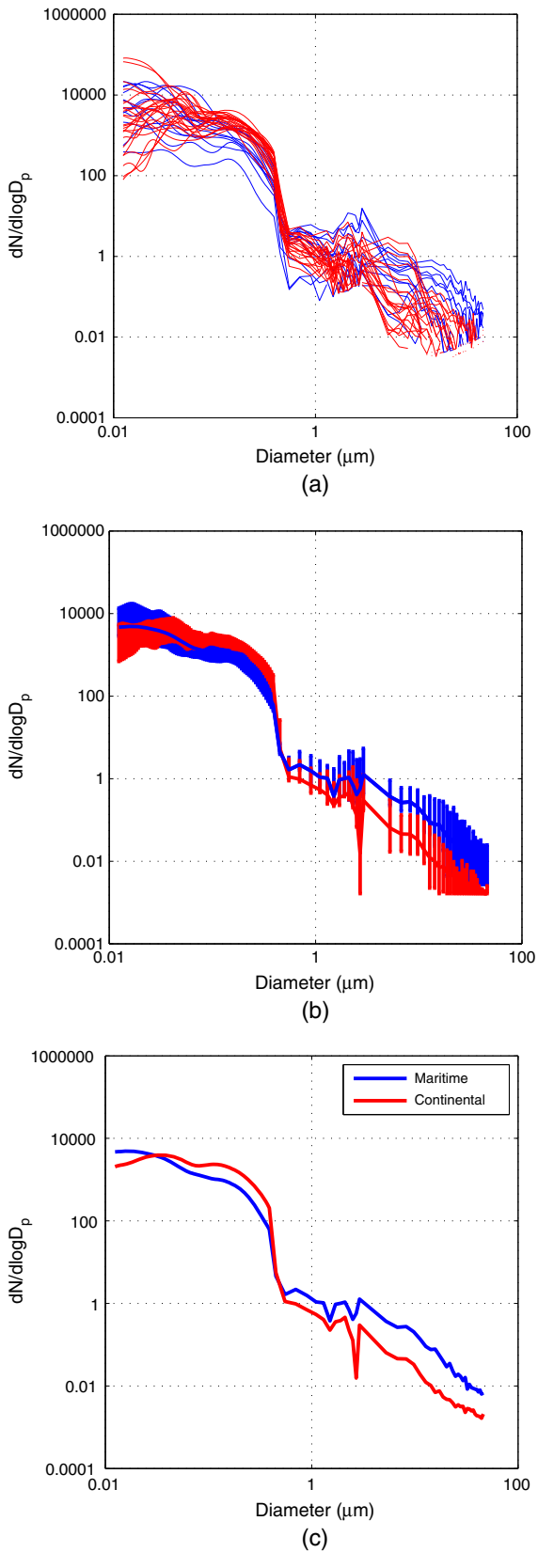

Figure 12. (a) Aerosol size spectra for the (blue) maritime and (red) continental regimes and (b, c) the mean spectra for each regime. Whiskers denote the range of 25th and 75thth percentile for each regime in Figure 12b but have been removed for clarity in Figure 12c.

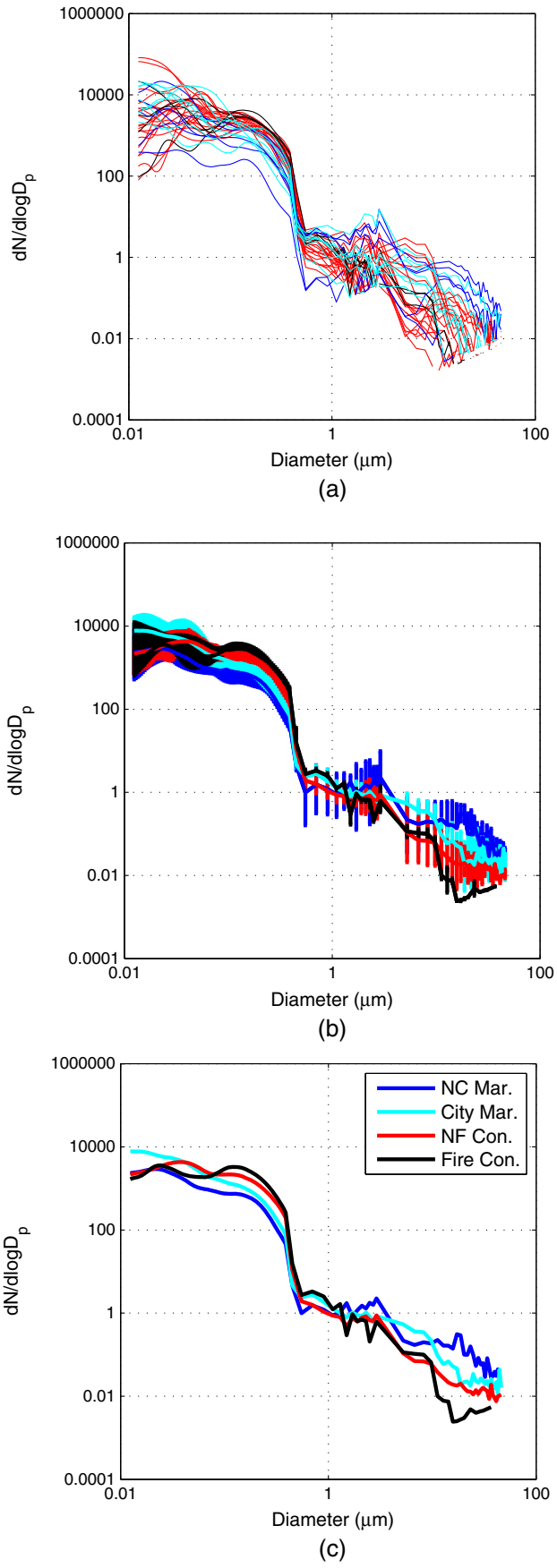

Figure 13. Same as in Figure 11, except for the four subregimes (see color legend).

Table 3. Average Cloud Droplet Concentrations (Conc), Mean Diameter (Diam), and Concentrations of Droplets Greater Than 20 μm (Conc > 20) by Regime for Each of the Three Calculation Methods. [a]Standard deviations (StdDev) and *p* values are also provided

Method	Regime	Conc	StdDev	*p*	Diam	StdDev	*p*	Conc > 20	StdDev	*p*
Steady state	MAR	411	135	.94	12.1	1.7	.13	5.9	7.8	.03
	CON	431	111		11.1	0.8		1.7	1.5	
Maximum	MAR	596	62	.30	11.1	1.2	.54	4.0	5.2	.65
	CON	534	113		11.1	0.8		2.6	3.6	
BinMax	MAR	353	207	.41	12.8	2.3	.01	7.9	9.0	.08
	CON	414	154		10.9	1.6		3.4	7.7	

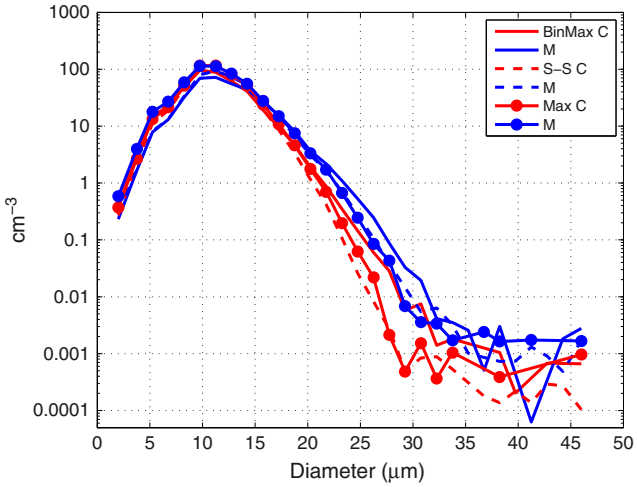

Figure 14. Mean cloud droplet spectra measured at 300–600 m above cloud base for each regime (continental = red, maritime = blue) and each calculation method (see legend).

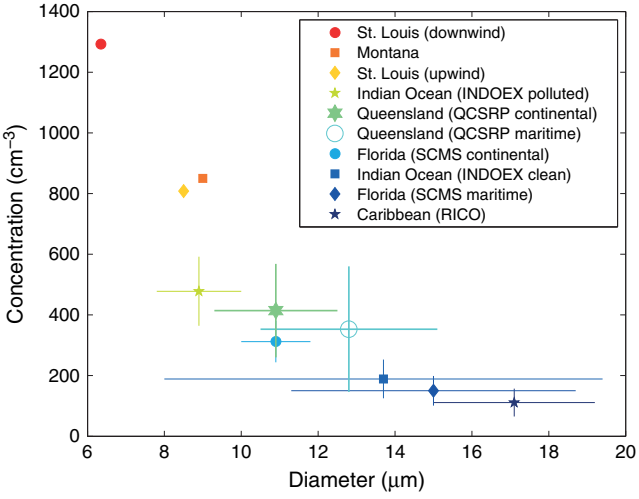

Figure 15. Graphical depiction of typical cloud base droplet concentrations and mean diameters measured in previous studies compared to the binmax results of the present study [adapted from *Tessendorf et al.*, 2012, Table 2]. Whiskers indicate ±1 standard deviation, when available in the given study.

typical of coastal or transitional locations, such as continental Florida or polluted areas of the Indian Ocean (Figure 15) [*Hudson and Yum*, 2001, 2002].

5. Supersaturation Calculations

[37] In order to investigate the observed similarities between the maritime and continental regimes' initial droplet concentrations, despite their differing aerosol and CCN concentrations, we have calculated the theoretical supersaturations that could have been attained. Using the data from the CCN supersaturation cycles, it is possible to determine the constant values in the CCN activity spectrum given by *Twomey* [1959] as

$$N = C(S-1)^k \tag{4}$$

where N is the total number concentration of CCN, C is the constant for number concentration of CCN particles (that represents an extrapolation of the CCN concentration at 1% SS), and k is the slope index. Although the CCN cycles were nominally run at 0.3%, 0.5%, and 0.8% SS, not every cycle actually stabilized temperatures at the specified supersaturation. Therefore, the temperature difference within the column was used to calculate the actual supersaturation for each measurement. Furthermore, only measurements taken once the temperature differential had stabilized were used in this analysis.

[38] A total of eight maritime and nine continental CCN cycles were used to determine the regime average CCN activity spectrum constants. Similar to past studies [e.g., *Twomey*, 1959; *Twomey and Wojciechowski*, 1969], our measurements showed that C and k are both lower in maritime clouds compared to continental. We calculated median C values of 397 cm^{-3} for maritime and 1036 cm^{-3} for continental clouds, and a median slope index (k) for maritime clouds of 0.75 compared to 0.97 for continental measurements.

5.1. Theoretical Maximum Supersaturation

[39] *Twomey* [1959, 1977] provides an estimate for theoretical maximum supersaturation at specific cloud base conditions, given as

$$(S-1)_{\max} = \left[2A^{3/2} w_u^{3/2} \Big/ BG^{1/2} CkB\left(\tfrac{k}{2}, \tfrac{3}{2}\right) \right]^{\frac{1}{k+2}} \tag{5}$$

where C and k are defined as above; w_u is the updraft velocity; $B(k/2,3/2)$ is the complete beta function; and the A, B, and G parameters are composed of state parameters, air and water constants, and the cloud base height and temperature. Using the mean values for C and k found for the maritime and continental regimes above, as well as the regime average cloud base heights and temperatures (Table 4), the theoretical maximum supersaturation for each regime was calculated at a

Table 4. Average Parameters for Each Regime Used in Equation (5)

Parameter	Maritime	Continental
Cloud base height (m)	889	1319
Cloud base temperature (°C)	18.25	17.15
C, CCN concentration extrapolated to 1% SS (cm^{-3}), from equation (4)	397	1036
k, slope index from equation (4)	0.75	0.97

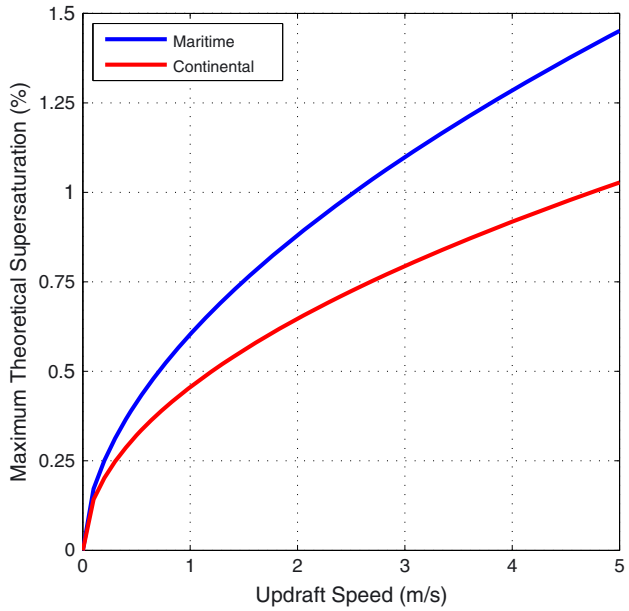

Figure 16. Maritime and continental theoretical maximum supersaturations according to equation (5).

variety of updraft speeds, shown in Figure 16. Under these assumptions and at a constant updraft speed, the maritime regime has the potential for greater supersaturations than the continental regime. This difference in potential supersaturation is mostly attributed to the different C and k parameters for the given regime.

5.2. "Actual" Supersaturation

[40] Where possible, the CCN measurements were paired with measurements of drop concentration between 300 and 600 m above cloud base (using the steady state method for this analysis). Using the individual flight values for C and k and the maximum cloud base drop concentration as N, equation (4) was used to calculate the "actual" supersaturation in the cloud. The maritime and continental averages were 0.77% and 0.55%, respectively.

[41] Despite having lower aerosol and CCN concentrations, the maritime drop concentrations were very similar to those found in continental air masses in the region. From these calculations, we conclude that the maritime clouds experienced higher supersaturations than their continental counterparts, on average, and thus were able to activate a higher fraction of aerosol particles.

6. Summary

[42] The goal of this study was to document representative cloud base aerosol conditions in the southeast Queensland region and investigate the relationship between the cloud base aerosol and initial cloud droplet spectra to establish implications of the aerosol on the cloud microphysics. Such representations could then be used to initialize models to further study potential aerosol impacts on precipitation formation in the region.

[43] Two general regimes were identified with maritime versus continental influences based on the hours each measurement's back trajectory spent over land. However, within each of these two regimes there was still substantial variability in aerosol concentration that was determined to be related to other factors, such as proximity to Brisbane or proximity to fires. Furthermore from these measurements, a regression model was developed that could be used for future radar analysis and cloud seeding operations in the region, in the absence of in situ aerosol measurements. Representative mean aerosol and cloud droplet spectra were also presented for each regime, which could be used as guidance in initializing and validating cloud resolving models. Finally, the somewhat surprising result that both the maritime and continental regimes had similar initial droplet concentrations (especially the cases using the steady state and max calculation methods) despite having significantly different aerosol concentrations could be attributed to the maritime regime inherently achieving a higher supersaturation. This would allow for a higher fraction of the aerosol particles to activate and form droplets, raising the droplet concentrations to levels more similar to the continental regime.

[44] The thermodynamic environments of the continental and maritime regimes were quite similar in instability and total precipitable water; however, the total *potential* instability was often higher in the continental regime. This was most likely because the midlevel trade wind inversion present in the maritime regime limited total CAPE values. The CAPE near cloud base (between 0 and 3 km) was much more similar between the two regimes. The most notable difference between the regimes was in the cloud base heights, which were consistently lower in the maritime regime. This environmental influence on the clouds that formed under the maritime regime could have contributed to the higher concentrations of coarse mode aerosol particles by nature of the measurements being taken closer to the ground surface. Our initial cloud base droplet spectra often tended to have a tail of larger drops in the maritime regime compared to the continental regime, which could be the result of the differing coarse mode aerosol concentrations. Furthermore, the aerosol spectra in the city-influenced maritime regime had the highest concentration of nucleation mode particles, which may have been attributed to the influence of city pollutants.

[45] Sorting out the relative importance of thermodynamics from aerosol effects is one of the biggest challenges in aerosol-cloud interaction studies. By having defined these

aerosol regimes in a quantitative way, we hope that future observational studies in the region can further diagnose the potential effects of the aerosol regimes and that numerical modeling studies can help fill in the gaps where our observations are incomplete and unable to control for aerosol differences alone.

[46] **Acknowledgments.** This research was sponsored by the Queensland Government Department of Environment and Resource Management through the Queensland Climate Change Centre of Excellence. The authors gratefully acknowledge the NOAA Air Resources Laboratory (ARL) for the provision of the HYSPLIT transport and dispersion model used in this publication. MODIS fire data were processed and provided by Christine Wiedinmyer (NCAR).

References

Barlow, A.K., and J. Latham (1983), A laboratory study of the scavenging of submicron aerosol by charged raindrops. *Q. J. R. Meteorol. Soc.*, *109*, 763–770.

Baumgardner, D., H. Jonsson, W. Dawson, D. O'Connor, and R. Newton (2001), The cloud, aerosol and precipitation spectrometer (CAPS): A new instrument for cloud investigations, *Atmos. Res.*, *59–60*, 251–264.

Bigg, E.K. (2008), Trends in rainfall associated with sources of air pollution. *Environ. Chem.*, *5*, 184–193. doi:10.1071/EN07086.

Collins, D. R., A. Nenes, R. C. Flagan, and J. H. Seinfeld (2000), The scanning flow DMA. *J. Aerosol Sci.*, *31*, 1129–1144.

Collins, D. R., D. R. Cocker, R. C. Flagan, and J. H. Seinfeld (2004), The scanning DMA transfer function. *Aerosol Sci. Technol.*, *38*, 833–850.

Draxler, R.R., and G.D. Rolph (2010), HYSPLIT (HYbrid Single-Particle Lagrangian Integrated Trajectory) Model Access via NOAA ARL READY Website (http://ready.arl.noaa.gov/HYSPLIT.php). NOAA Air Resources Laboratory, Silver Spring, MD.

Dye, J.E., and D. Baumgardner (1984), Evaluation of the forward scattering spectrometer probe: I. Electronic and optical studies. *J. Atmos. Oceanic Technol.*, *1*, 329–344.

Dye, J.E., J.J. Jones, W.P. Winn, T.A. Cerni, B. Gardiner, D. Lamb, R.L. Pitter, J. Hallett, and C.P.R. Saunders (1986), Early electrification and precipitation development in a small, isolated Montana cumulonimbus. *J. Geophys. Res.*, *91*, 1231–1247.

Feingold, G., W.R., Cotton, S.M. Kreidenweis, and J.T. Davis (1999), The impact of giant cloud condensation nuclei on drizzle formation in stratocumulus: Implications for cloud radiative properties, *J. Atmos. Sci.*, *56*, 4100–4117.

Fitzgerald, J.W., and P.A. Spyers-Duran (1973), Changes in cloud nucleus concentration and cloud droplet size distribution associated with pollution from St. Louis. *J. Appl. Meteorol.*, *12*, 511–516.

Freud, E., J. Strom, D. Rosenfeld, P. Tunved, E. Swietlicki (2008), Anthropogenic aerosol effects on convective cloud microphysical properties in southern Sweden, *Tellus B Chem. Phys. Meteorol.*, *2*, 286–297.

Giglio, L., J. Descloitres, C.O. Justice, and Y.J. Kaufman (2003), An enhanced contextual fire detection algorithm for MODIS. *Remote Sens. Environ.*, *87*, 273–282.

Hudson, J.G., and S. S. Yum (2001), Maritime-continental drizzle contrasts in small cumuli. *J. Atmos. Sci.*, *58*, 915–926.

Hudson, J.G., and S. S. Yum (2002), Cloud condensation nuclei spectra and polluted and clean clouds over the Indian Ocean. *J. Geophys. Res.*, *107*, doi:10.1029/2001JD000829.

Hudson, J.G., and S. Mishra (2007), Relationships between CCN and cloud microphysics variations in clean maritime air. *Geophys. Res. Lett.*, *34*, doi:10.1029/2007GL030044.

Hudson, J.G., S. Noble, V. Jha, and S. Mishra (2009), Correlations of small cumuli droplet and drizzle drop concentrations with cloud condensation nuclei concentrations, *J. Geophys. Res.*, *114*, D05201, doi:10.1029/2008JD010581.

Hudson, J.G., S. Noble, and V. Jha (2010), Stratus cloud supersaturations. *Geophys. Res. Lett.*, *37*, L21813, doi:10.1029/2010GL045197.

Hudson, J.G., V. Jha, and S. Noble (2011), Drizzle correlations with giant nuclei. *Geophys. Res. Lett.*, *38*, L05808, doi:10.1029/2010GL046207.

IPCC (2007), Climate Change 2007: The Physical Science Basis. Contribution of Working Group I to the Fourth Assessment Report of the Intergovernmental Panel on Climate Change [Solomon, S., D. Qin, M. Manning, Z. Chen, M. Marquis, K.B. Averyt, M. Tignor and H.L. Miller (eds.)]. Cambridge University Press, Cambridge, UK and New York, NY, USA.

Kerker, M., and V. Hampl (1974), Scavenging of aerosol particles by a falling water drop and calculation of washout coefficients. *J. Atmos. Sci.*, *31*, 1368–1376.

Khain A., D. Rosenfeld, and A. Pokrovsky (2005), Aerosol impact on the dynamics and microphysics of deep convective clouds. *Q. J. R. Meteorol. Soc.*, *131*, 2639–2663.

Lilliefors, H. (1967), On the Kolmogorov–Smirnov test for normality with mean and variance unknown, *J. Am. Stat. Assoc.*, *62*. pp. 399–402.

Miller, R.C. (1972), Notes on analysis and severe storm forecasting procedures of the Air Force Global Weather Central. Tech. Rept. 200 (R), Headquarters, Air Weather Service, USAF, 190 pp.

Roberts, G.C., and A. Nenes,(2005), A continuous-flow streamwise thermal-gradient CCN chamber for atmospheric measurements. *Aerosol Sci. Technol.*, *3*, 206–221.

Rosenfeld, D. (1999), TRMM observed first direct evidence of smoke from forest fires inhibiting rainfall. *Geophys. Res. Lett.*, *26*, 3105–3108.

Rosenfeld, D. (2000), Suppression of rain and snow by urban and industrial air pollution. *Science*, *287*, 1793–1796.

Rosenfeld, D., U. Lohmann, G.B. Raga, C.D. O'Dowd, M. Kulmala, S. Fuzzi, A. Reissell, and M.O. Andreae (2008), Flood or drought: How do aerosols affect precipitation? *Science*, *321*, 1309–1313.

Squires, P. (1958), The microstructure and colloidal stability of warm clouds. I. The relation between structure and stability, *Tellus*, *10*, 256–271.

Tao, W.-K., X. Li, A. Khain, T. Matsui, S. Lang, and J. Simpson (2007), Role of atmospheric aerosol concentration on deep convective precipitation: Cloud-resolving model simulations. *J. Geophys. Res.*, *112*, doi 10.1029/2007JD008728.

Tessendorf, S.A., et al. (2010), Overview of the Queensland Cloud Seeding Research Program. *J. Weather Modif.*, *42*, 33–48.

Tessendorf, S.A., et al. (2012), The Queensland Cloud Seeding Research Program. *Bull. Am. Meteorol. Soc.*, *93*, 75–90.

Twomey, S. (1959), The nuclei of natural cloud formation. Part II: The supersaturation in natural clouds and the variation of cloud droplet concentration. *Geofis. Pura Appl.*, *43*, 243–249.

Twomey, S. (1977), Atmospheric Aerosols. Elsevier, 302 pp.

Twomey, S., and T. A. Wojciechowski (1969), Observations of the geographical variation of cloud nuclei. *J. Atmos. Sci.*, *26*, 648–688.

Warner, J. (1968), A reduction in rainfall associated with smoke from sugarcane fires—An inadvertent weather modification? *J. Appl. Meteorol.*, *7*, 247–251.

Warner, J., and S. Twomey (1967), The production of cloud nuclei by cane fires and the effect on cloud droplet concentration. *J. Atmos. Sci.*, *24*, 704–706.

Wiedinmyer, C. , B. Quayle, C. Geron, A. Belote, D. McKenzie, X. Zhang, S. O'Neill, and K.K. Wynne (2006), Estimating emissions from fires in North America for Air Quality Modeling. *Atmos. Environ.*, *40*, 3419–3432.

Yum, S.S., J.G. Hudson, and Y. Xie (1998), Comparisons of cloud microphysics with cloud condensation nuclei spectra over the summertime Southern Ocean. *J. Geophys. Res.*, *103*, 16,625–16,636.